

# Determination of symmetry energy from experimental and observational constraints; prediction on CREX

Shingo Tagami,<sup>1</sup> Nobutoshi Yasutake,<sup>2,3</sup> Mitsunori Fukuda,<sup>4</sup> Jun Matsui,<sup>1</sup> and Masanobu Yahiro<sup>1,\*</sup>

<sup>1</sup>*Department of Physics, Kyushu University, Fukuoka 812-8581, Japan*

<sup>2</sup>*Department of Physics, Chiba Institute of Technology, Chiba 275-0023, Japan*

<sup>3</sup>*Advanced Science Research Center, Japan Atomic Energy Agency, Ibaraki 319-1195, Japan*

<sup>4</sup>*Department of Physics, Osaka University, Osaka 560-0043, Japan*

(Dated: January 24, 2022)

Taking  $r_{\text{skin}}^{208}(\text{PREX}) = 0.33_{-0.18}^{+0.16}$  fm as an experimental constraint and  $M_{\max}^{\text{NS}} \geq 2M_{\text{sun}}$  as an observational (astrophysical) constraint, we determine an indisputable range for  $J$ ,  $L$ ,  $K_{\text{sym}}$  defined in Eq. (1). For this purpose, we take a statistical approach. We first accumulate the 206 EoS data from theoretical works and take correlation between  $r_{\text{skin}}^{208}$  and  $L$  for the 206 EoSs, where 7 Gogny EoSs are obtained by our calculations. Since the correlation coefficient is  $R = 0.99$ , we can regard  $L$  as a function of  $r_{\text{skin}}^{208}$ , so that we succeed in deducing an empirical constraint  $L = 31 - 161$  MeV from  $r_{\text{skin}}^{208}(\text{PREX}) = 0.15 - 0.49$  fm. For the 47 EoSs satisfying the observational constraint, 46 EoSs satisfy the empirical constraint. The 46 EoSs yield  $J = 29 - 44$  MeV,  $L = 37 - 135$  MeV,  $K_{\text{sym}} = (-137) - (160)$  MeV. This is a primary result. When we take correlation between  $r_{\text{skin}}^{48}$  and  $r_{\text{skin}}^{208}$  for the 206 EoSs,  $R$  is 0.99. The  $r_{\text{skin}}^{48}$ - $r_{\text{skin}}^{208}$  relation allows us to transform  $r_{\text{skin}}^{208}(\text{PREX})$  into the corresponding data on  $r_{\text{skin}}^{48}$ . In order to estimate a value of  $r_{\text{skin}}^{48}$  for ongoing CREX, we take the weighted mean and its error of two present data on  $r_{\text{skin}}^{48}$  and transformed PREX value on  $r_{\text{skin}}^{48}$ . The weighted mean is  $r_{\text{skin}}^{48} = 0.17$  fm. This is a prediction for the central value of CREX.

## I. INTRODUCTION AND CONCLUSION

*Background:* For the symmetry energy  $S_{\text{sym}}(\rho)$  as a function of nuclear density  $\rho$ , many predictions have been made so far. The  $S_{\text{sym}}(\rho)$  is expanded around the nuclear-matter saturation density  $\rho_0$ :

$$S_{\text{sym}}(\rho) = J + \frac{L(\rho - \rho_0)}{3\rho_0} + \frac{K_{\text{sym}}(\rho - \rho_0)^2}{18\rho_0^2} + \dots \quad (1)$$

for the symmetry energy  $J \equiv S_{\text{sym}}(\rho)$ , the slope  $L$  and the curvature  $K_{\text{sym}}$  at  $\rho = \rho_0$ . The  $S_{\text{sym}}(\rho)$  were determined from some experimental and observational constraints and their combinations. It is important which constraint is selected, particularly for neutron stars (NSs).

The  $S_{\text{sym}}(\rho)$  itself cannot be measured by experiments. In place of  $S_{\text{sym}}(\rho)$ , the neutron-skin thickness  $r_{\text{skin}}$  is measured to determine  $L$ , since the strong correlation between  $r_{\text{skin}}^{208}$  and  $L$  is well known [1, 2]. The direct measurement on  $r_{\text{skin}}^{208}$  is the Lead Radius EXperiment (PREX) composed of parity-violating and elastic electron scattering; the neutron radius  $r_n$  is determined from the former experiment, whereas the proton radius  $r_p$  is from the latter. The weak and electromagnetic measurement provides  $r_n^{208} = 5.78_{-0.18}^{+0.16}$  fm [3, 4] that yields

$$r_{\text{skin}}^{208}(\text{PREX}) = 0.33_{-0.18}^{+0.16} \text{ fm} \quad (2)$$

under  $r_p^{208} = 5.45$  fm. The  $r_{\text{skin}}^{208}(\text{PREX})$  has a large error. For this reason, the PREX-II and the  $^{48}\text{Ca}$  Radius EXperiment (CREX) are ongoing at Jefferson Lab [4]. As

for  $^{48}\text{Ca}$ , Hagen *et al.* obtained a value of proton radius  $r_p$  with the coupled-cluster calculation with the chiral interaction [5]. Using the  $J-r_p$  and  $L-r_p$  correlations, they have showed  $25.2 \lesssim J \lesssim 30.4$  MeV and  $37.8 \lesssim L \lesssim 47.7$  MeV, where the theoretical errors of  $J$  and  $L$  mainly come from the systematic uncertainties of the employed Hamiltonians.

The  $S_{\text{sym}}(\rho)$  influences strongly the nature within NSs. For a pulsar in a binary system, detection of the general relativistic Shapiro delay allows us to determine the mass  $M$  of NS. In fact, the NS with  $M = 1.97 \pm 0.04 M_{\text{sun}}$  is observed [6]. In  $\rho = 2 - 3 \rho_0$ , the strangeness changing weak decay replaces nucleons by hyperons. The decay makes the maximum mass  $M_{\max}$  decrease, if the decay occurs really. In this paper, we assume the decay does not take place, because nucleon-hyperon and hyperon-hyperon interactions are still unknown. As an essential constraint on the EoS from astrophysics, one can consider

$$M_{\max} \geq 2 M_{\text{sun}}, \quad (3)$$

where  $M_{\max}$  is the maximum mass of NS and  $M_{\text{sun}}$  is the solar mass.

*Aims and conclusion:* The first aim is to determine an indisputable range for  $J$ ,  $L$  and  $K_{\text{sym}}$  from  $r_{\text{skin}}^{208}(\text{PREX}) = 0.33_{-0.18}^{+0.16}$  fm as an experimental constraint and  $M_{\max}^{\text{NS}} \geq 2M_{\text{sun}}$  as an observational (astrophysical) constraint. Our result is  $J = 29 - 44$  MeV,  $L = 37 - 135$  MeV,  $K_{\text{sym}} = (-137) - (160)$  MeV.

For the first aim, we take a statistical approach. We first take a correlation between  $r_{\text{skin}}^{208}$  and  $L$ . The number of EoSs should be large for obtaining reliable correlation statistically. We then accumulate 204 EoSs from theoretical works and construct 2 Gogny-type EoSs, so that we get 206 EoSs. An advantage of this statistical analysis is to eliminate systematic error for the correlation

\* orion093g@gmail.com

between  $r_{\text{skin}}^{208}$  and  $L$ . The procedure of the statistical analysis is as follows.

1. We take Eq. (2) as an essential experimental constraint and Eq. (3) as an essential observational constraint.
2. In order to take reliable correlation between  $r_{\text{skin}}^{208}$  and  $L$ , we accumulate 204 EoS data from theoretical works [2, 7–31] and construct 2 Gogny-type EoSs in which  $r_{\text{skin}}^{208}$  and/or  $L$  is presented. The 206 EoSs are presented in Table I. The correlation function between  $r_{\text{skin}}^{208}$  and  $L$  is obtained self-consistently; the starting correlation function is determined from the EoSs in which  $r_{\text{skin}}^{208}$  and  $L$  are provided. The resulting correlation function has  $R = 0.99$ , while the starting correlation function does  $R = 0.98$ . Since the resulting correlation is perfect, we refer to the resulting correlation as “the  $r_{\text{skin}}^{208}$ – $L$  relation”. In other words,  $L$  is a function of  $r_{\text{skin}}^{208}$ ; see Fig. 1. Using the  $L$ – $r_{\text{skin}}^{208}$  relation, we get an empirical constraint  $L_{\text{empirical}} = 31 - 161$  from  $r_{\text{skin}}^{208}$  (PREX).
3. For 7 Gogny-type EoSs in Table I, both  $r_{\text{skin}}^{208}$  and  $L$  are not calculated. We then calculate  $J$ ,  $L$ ,  $K_{\text{sym}}$  with the energy density functional and  $r_{\text{skin}}^{48}$  and  $r_{\text{skin}}^{208}$  with the Hartree-Fock-Bogoliubov method with the angular momentum projection. Two of 7 EoSs are newly constructed.
4. The 184 EoSs satisfying  $L_{\text{empirical}} = 31 - 161$  in Table I yield  $J = 28 - 44$  MeV,  $L = 31 - 161$  MeV,  $K_{\text{sym}} = (-266) - (235)$  MeV.
5. Table III shows the 47 EoSs satisfying the observational constraint (3). 46 EoSs satisfying  $L_{\text{empirical}} = 31 - 161$  in Table III give  $J = 29 - 44$  MeV,  $L = 37 - 135$  MeV,  $K_{\text{sym}} = (-137) - (160)$  MeV. These are indisputable ranges of  $J$ ,  $L$ ,  $K_{\text{sym}}$ .

The second aim is to estimate a central value of CREX. We find that the correlation between  $r_{\text{skin}}^{48}$  and  $r_{\text{skin}}^{208}$  is perfect, because  $R = 0.99$ . The  $r_{\text{skin}}^{48}$ – $r_{\text{skin}}^{208}$  relation allows us to transform  $r_{\text{skin}}^{208}$  (PREX) into the corresponding range on  $r_{\text{skin}}^{48}$ . We then take the weighted mean and its error of two data [32, 33] measured for  $r_{\text{skin}}^{48}$  and the transformed  $r_{\text{skin}}^{208}$  (PREX). The weighted mean is a prediction on the central value of CREX; namely,

$$r_{\text{skin}}^{48}(\text{CREX}) = 0.17 \text{ fm}. \quad (4)$$

We show the statistical analysis and its results in Sec. II and our estimate for the central value of CREX in Sec. III. Discussions are made in Sec. IV.

## II. THE STATISTICAL ANALYSIS AND ITS RESULTS

### A. Sample data of 206 EoSs

We first accumulate 204 EoSs from theoretical works [2, 7–31] in which  $r_{\text{skin}}^{208}$  and/or  $L$  is presented. In the 204 EoSs of Table I, both  $r_{\text{skin}}^{208}$  and  $L$  are not presented for 5 Gogny-type EoSs (D1S, D1N, D1M, D1M\*, D1P). We then construct 2 Gogny-type EoSs, D1MK and D1PK, in which strong three-body forces are into account. Eventually, we get the 206 EoSs, as shown in Table I. Now, we make three comments for Table I.

1. For D1S, D1N, D1M, D1M\*, D1MK, D1P, D1PK, we calculate  $r_{\text{skin}}^{208}$  and  $r_{\text{skin}}^{48}$  with the Hartree-Fock-Bogoliubov method with the angular momentum projection. For the Gogny EoSs, the effective nucleon-nucleon interaction can be described as

$$\begin{aligned} V(\vec{r}) = & \sum_{i=1,2} t_0^i (1 + x_0^i P_\sigma) \rho^{\alpha_i} \delta(\vec{r}) \\ & + \sum_{i=1,2} (W_i + B_i P_\sigma - H_i P_\tau - M_i P_\sigma P_\tau) e^{-\frac{r^2}{\mu_i^2}} \\ & + i W_0 (\sigma_1 + \sigma_2) [\vec{k}' \times \delta(\vec{r}) \vec{k}], \end{aligned} \quad (5)$$

where  $\sigma$  and  $\tau$  are the Pauli spin and isospin operators, respectively, and the corresponding exchange operators  $P_\sigma$  and  $P_\tau$  are defined as usual. See Table II for the parameter sets of D1MK and D1PK. For matter, the energy density functional is used.

2. Dutra *et al.* selected 16 EoSs from 240 Skyrme EoSs by using a series of criteria [23]. The 16 EoSs ( GSkiI, GSkiII, KDE0v1, LNS, MSL0, NRAPR, Ska25s20, Ska35s20, SKRA, SkT1, SkT2, SkT3, Skxs20, SQMC650, SQMC700, SV-sym32) are in Table I.
3. Out of the 240 Skyrme EoSs, Tsang *et al.* selected 12 EoSs (KDE0v1, NRAPR, Ska25, Ska35, SKRA, SkT1, SkT2, SkT3, SQMC750, SV-sym32, Sly4, SkM\*) and fitted them to nuclear binding energies, charge radii and single-particle energies [8]. The fitted set is identified with the label “-T” from the original set. Brown and Schwenk fitted the original set so that the effective mass  $m^*/m$  can be 0.9 in neutron matter at  $\rho = 0.10 \text{ fm}^{-3}$  [24]. This set is identified with the label by “-B”. The three sets are in Table I.

### B. $L$ as a function of $r_{\text{skin}}^{208}$

As a correlation coefficient  $R$  between two variables  $X$  and  $Y$ , we take

$$R = \frac{\sigma_{XY}}{\sigma_X \sigma_Y} \quad (6)$$

for the covariance  $\sigma_{XY}$  between  $X$  and  $Y$  and the standard deviation  $\sigma_X$  of  $X$ .

Figure 1 shows correlations between  $r_{\text{skin}}^{208}$  and each of  $J$ ,  $L$ ,  $K$ ,  $K_{\text{sym}}$  for 206 EoSs of Table I, where  $K$  and  $K_{\text{sym}}$  are the incompressibility and the symmetry-energy incompressibility, respectively. Four dotted lines denote

$$L = 618.24 r_{\text{skin}}^{208} - 57.399 \quad (7)$$

for the correlation between  $L$  and  $r_{\text{skin}}^{208}$ ,

$$J = 48.287 r_{\text{skin}}^{208} + 23.091 \quad (8)$$

for the correlation between  $J$  and  $r_{\text{skin}}^{208}$ ,

$$K_{\text{sym}} = 1838.2 r_{\text{skin}}^{208} - 446.57 \quad (9)$$

for the correlation between  $K_{\text{sym}}$  and  $r_{\text{skin}}^{208}$

$$K = 206.24 r_{\text{skin}}^{208} + 201.82 \quad (10)$$

for the correlation between  $K_{\text{sym}}$  and  $r_{\text{skin}}^{208}$ , respectively. The correlation coefficient is  $R = 0.98$  for  $L$ ,  $R = 0.74$  for  $J$ ,  $R = 0.84$  for  $K_{\text{sym}}$ ,  $R = 0.30$  for  $K$ . Among the four correlations, only the correlation (7) between  $L$  and  $r_{\text{skin}}^{208}$  can be regarded as a function, since the  $R$  is perfect.

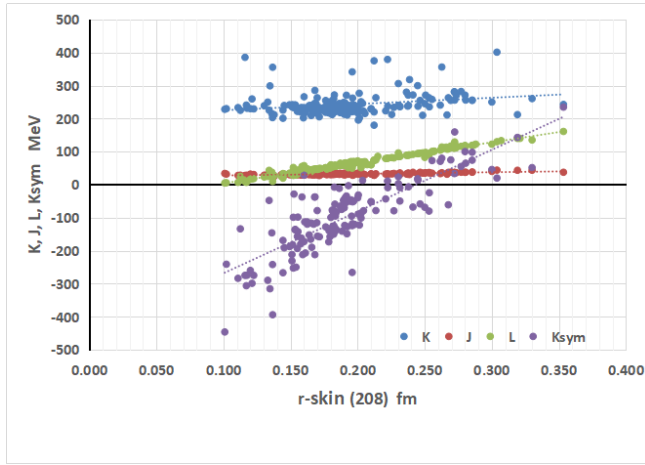


FIG. 1. Properties ( $J$ ,  $L$ ,  $K$ ,  $K_{\text{sym}}$ ) of 206 EoSs (dotted). Four dotted lines stand for correlations between  $r_{\text{skin}}^{208}$  and each of  $J$ ,  $L$ ,  $K$ ,  $K_{\text{sym}}$ .

In order to obtain both  $L$  and  $r_{\text{skin}}^{208}$  for all of the 206 EoSs, we take a self-consistent way where the starting function is Eq. (7). The resulting function

$$L(r_{\text{skin}}^{208}) = 620.39 r_{\text{skin}}^{208} - 57.963 \quad (11)$$

has  $R = 0.99$ . We refer to Eq. (11) as “the  $r_{\text{skin}}^{208}$ - $L$  relation”.

### C. Empirical constraint on $L$

Using the  $r_{\text{skin}}^{208}$ - $L$  relation (11), we can get an empirical constraint

$$L_{\text{empirical}} = 31 - 161 \text{ MeV} \quad (12)$$

from the experimental constraint  $r_{\text{skin}}^{208}$ (PREX).

In Table I, 184 EoSs satisfy the empirical constraint (12) on  $L$ . For  $J$ ,  $L$ ,  $K_{\text{sym}}$ , the 184EoSs yield

$$J = 28 - 44, \quad L = 31 - 161, \quad K_{\text{sym}} = (-266) - (235) \quad (13)$$

in units of MeV.

### D. Observational and empirical constraints

In addition to the empirical constraint (12) on  $L$ , we take the observational constraint (3). The procedure is as follows.

In Table I, 47 EoSs satisfy the observational constraint (3); see Table III. Out of the 47 EoSs, the 46 (BSk25, BSk20, BSk26, D1M\*, Sly230a, D2, SLy4, BSk24, BSk21, SFHo, Sly2, SKb, DD-ME2, Sly9, D1PK, DD-ME1, HS(DD2), NL3 $\omega\rho$ , APR(E0019), BSk23, SkI6, SkI4, FSUgold2.1, BSR2, SGI, D1AS, BSk22, SkMP, LS220, LS375, SKa, Rs, TFa, BSR6, TMA(E0008), SK272, GM1, SK255, SV, SkI3, SkI2, TM1, NL3, TFb, SKI5, TFc) satisfy the empirical constraint (12) on  $L$ . We take  $J$ ,  $L$ ,  $K_{\text{sym}}$  from the 46 EoS. The results are

$$J = 29 - 44, \quad L = 37 - 135, \quad K_{\text{sym}} = (-137) - (160) \quad (14)$$

in units of MeV. This is our primary result for  $J$ ,  $L$ ,  $K_{\text{sym}}$ , since we use Eq. (2) as an essential experimental constraint and Eq. (3) as an essential observational constraint.

## III. PREDICTION FOR CREX

### A. Experimental data on $r_{\text{skin}}^{48}$

At the present stage, there are two good measurements for  $r_{\text{skin}}^{48}$ . The high-resolution measurement of  $\alpha_D$  was applied for  $^{48}\text{Ca}$  in RCNP [32]: the data is

$$r_{\text{skin}}^{48}(\text{RCNP}) = 0.14 - 0.20 \text{ fm}. \quad (15)$$

Very lately, Tanaka *et al.* determined

$$r_{\text{skin}}^{48}(\text{RIKEN}) = 0.146 \pm 0.06 \text{ fm} \quad (16)$$

by measuring interaction cross sections for  $^{48}\text{Ca}$  scattering on a C target in RIKEN [33].

### B. Relation between $r_{\text{skin}}^{48}$ and $r_{\text{skin}}^{208}$

For the 206 EoSs in Table I, we take correlation between  $r_{\text{skin}}^{48}$  and  $r_{\text{skin}}^{208}$  for the EoSs in which both  $r_{\text{skin}}^{48}$  and  $r_{\text{skin}}^{208}$  are presented. The correlation coefficient is perfect because of  $R = 0.98$ . In order to yield values of  $r_{\text{skin}}^{48}$  and  $r_{\text{skin}}^{208}$  for all of 206 EoSs, we take correlation between  $r_{\text{skin}}^{48}$  and  $r_{\text{skin}}^{208}$  self-consistently: the starting  $r_{\text{skin}}^{48}$ - $r_{\text{skin}}^{208}$  relation is obtained from the EoSs in which  $r_{\text{skin}}^{48}$  and  $r_{\text{skin}}^{208}$

are presented. Since the resulting relation has  $R = 0.98$ , we succeed in obtaining  $r_{\text{skin}}^{48}$  as a function of  $r_{\text{skin}}^{208}$ . The function thus obtained is

$$r_{\text{skin}}^{48}(r_{\text{skin}}^{208}) = 0.5547 r_{\text{skin}}^{208} + 0.0718; \quad (17)$$

see Fig. 2.

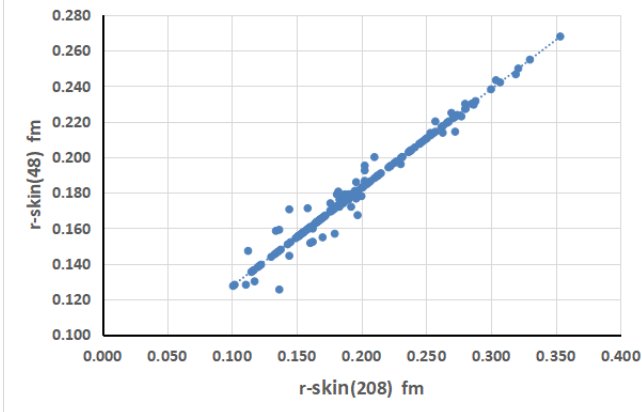


FIG. 2. Relation between  $r_{\text{skin}}^{48}$  and  $r_{\text{skin}}^{208}$ . The dotted line stands for Eq. (17), while dots correspond to 206 EoSs.

### C. Data on $r_{\text{skin}}^{48}$ transformed from $r_{\text{skin}}^{208}$ (PREX)

Transforming the data  $r_{\text{skin}}^{208}$ (PREX) into the corresponding data on  $r_{\text{skin}}^{48}$ , we get

$$r_{\text{skin}}^{48}(\text{tPREX}) = 0.25 \pm 0.09 \text{ fm}. \quad (18)$$

The transformed data (19) is consistent with the original ones (15) and (16).

Taking the weighted mean and its error of Eqs. (15), (16), (19), we get

$$r_{\text{skin}}^{48}(\text{RCNP \& RIKEN \& tPREX}) = 0.17 \pm 0.03 \text{ fm}. \quad (19)$$

We then regard 0.17 fm as an estimate for the central value of CREX. The derivation 0.03 fm is based on the “maximum likelihood”, in which we assume that the kernels of prior probabilities on the measurements are independent Gaussian types. The details are shown in Appendix. Since the estimated error of CREX is 0.02 fm [4], the CREX group will show their result with similar accuracy in future.

## IV. DISCUSSIONS

### A. Astrophysical constraints

As for the astrophysical constraints, Horowitz summarized the other observational constraints and the lower limit of NS radius  $R$  determined from PREX [34]; his mention is illustrated in Fig. 3, with the mass-radius relations for our EoSs, D1MK and D1PK. Bauswein *et*

*al.* suggested that if  $1.6 M_{\text{sun}}$  stars have radii less than the indicated lower limit, the NS in GW170817 would collapse to soon to a black hole and not eject material enough to power the observed Kilonova [35]. When the maximum mass of a NS is above the red dotted line, Metzger *et al.* argued that the compact remnant in GW170817 lives too long and provides too much energy to the kilonova [36]. Finally the GW170817 limit on the radius of a  $1.4 M_{\text{sun}}$  is from the limit on the gravitational deformability [37, 38], whereas the limit on the EoS at low density from PREX is plotted as a minimum radius of a  $0.5 M_{\text{sun}}$  NS. Such low mass NSs have low central densities comparable to nuclear density.

In our calculations for the mass-radius relation, the beta-equilibrium is taken into account. Below the sub-nuclear density  $n < 0.1 \text{ fm}^{-3}$ , we use the BPS EoS [39]. Model D1PK satisfies the observable constraint (3). Meanwhile, the maximum mass  $M_{\text{max}} = 1.94 M_{\text{sun}}$  of D1MK is slightly smaller than the observable constraint (3), but is in the  $M = 1.97 \pm 0.04 M_{\text{sun}}$  of Ref. [6]. As an interesting result, Model D1PK satisfies all of the observation constraints mentioned above and the lower bound of  $R$  determined from PREX. Model D1MK almost satisfies the observation constraints mentioned above and the lower bound of  $R$  determined from PREX.

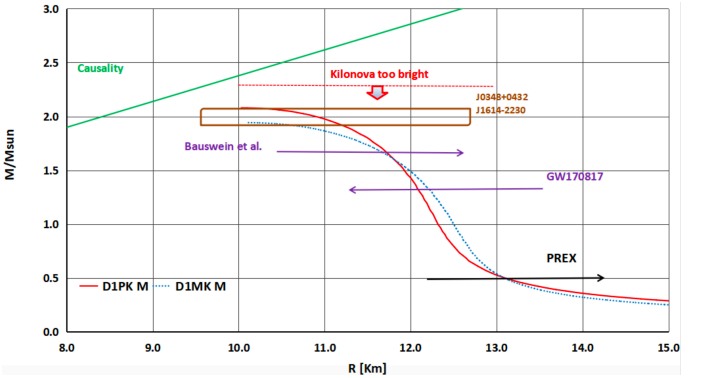


FIG. 3.  $M$ - $R$  relation for D1MK and D1PK. Model D1PK is shown by the solid line, and D1MK is by the dashed line. See the text for the observation constraints shown and the lower limit of  $R$  determined from PREX. The details are shown Ref. [34].

### ACKNOWLEDGMENTS

M. Y. expresses my gratitude to Dr. Y. R. Shimizu for his useful information. N. Yasutake is grateful to T. Inakura for the fruitful discussions. This work was supported by JSPS KAKENHI Grant Numbers 20K03951, 20H04742.

## Appendix A: Mean weighed method based on independent Gaussian priors

Here, we introduce how to estimate one unknown value  $X$  from some independent measurements. In this paper, the kernels of the the priors for the measurements are assumed to be Gaussian types. Then, the probability of  $i$ -th measurement with the physical value  $x_i$  is

$$P(x_i) \propto \frac{1}{\sigma_i} \exp[-(x_i - X)^2/(2\sigma_i^2)], \quad (\text{A1})$$

where  $\sigma_i$  is each dispersion.

Each measurement is assumed to be independent, therefore the probability  $P(x_A, x_B)$  to obtain two measurements  $x_A$  and  $x_B$ , for example, can be expressed as the product of each probability,

$$P(x_A, x_B) = P(x_A)P(x_B). \quad (\text{A2})$$

According to the maximum likelihood principle, we obtain the best estimation  $X_{\text{best}}$  for the unknown quantity, by taking the maximum value of  $P(x_A, x_B)$  respect to  $X$ , as

$$X_{\text{best}} = \frac{w_A x_A + w_B x_B}{w_A + w_B}, \quad (\text{A3})$$

where the weights  $w_A$  and  $w_B$  are given by

$$w_A = 1/\sigma_A^2, \quad w_B = 1/\sigma_B^2. \quad (\text{A4})$$

We can extend the above discussion to general cases with  $N$ -samples, then we obtain

$$X_{\text{best}} = \sum_{i=1}^N w_i x_i / \sum_{i=1}^N w_i, \quad (\text{A5})$$

where the weights  $w_i$  are related to the individual error distributions in a similar way,

$$w_i = 1/\sigma_i^2 \quad (i = 1, 2, \dots, N). \quad (\text{A6})$$

The standard deviation from the weighted mean,  $\sigma$ , is reobtained as

$$\sigma^2 = \frac{\sum_{i=1}^N w_i^2 (x_i - X_{\text{best}})^2 \sigma_i^2}{\left(\sum_{i=1}^N w_i\right)^2} = \frac{1}{\sum_{i=1}^N w_i} \quad (\text{A7})$$

The true value  $X$  is expressed in the form,

$$X = X_{\text{best}} \pm \sigma. \quad (\text{A8})$$

- 
- [1] B. A. Brown, Phys. Rev. Lett. **111**, no. 23, 232502 (2013), [arXiv:1308.3664 [nucl-th]].
  - [2] X. Roca-Maza, M. Centelles, X. Vinas and M. Warda, Phys. Rev. Lett. **106**, 252501 (2011), [arXiv:1103.1762 [nucl-th]].
  - [3] S. Abrahanyan *et al.*, Phys. Rev. Lett. **108**, 112502 (2012), [arXiv:1201.2568 [nucl-ex]].
  - [4] R. Michaels *et al.*, Lead Radius Experiment PREX proposal 2005; <http://hallaweb.jlab.org/parity/prex/>.
  - [5] G. Hagen *et al.*, Nature Phys. **12**, no. 2, 186 (2015), [arXiv:1509.07169 [nucl-th]].
  - [6] P. Demorest, T. Pennucci, S. Ransom, M. Roberts and J. Hessels, Nature **467**, 1081 (2010), [arXiv:1010.5788 [astro-ph.HE]].
  - [7] A. Akmal, V. R. Pandharipande and D. G. Ravenhall, Phys. Rev. C **58**, 1804 (1998), [nucl-th/9804027].
  - [8] C. Y. Tsang, B. A. Brown, F. J. Fattoyev, W. G. Lynch and M. B. Tsang, Phys. Rev. C **100**, no. 6, 062801 (2019), [arXiv:1908.11842 [nucl-th]].
  - [9] T. Inakura and H. Nakada, Phys. Rev. C **92**, 064302 (2015), [arXiv:1509.02982 [nucl-th]].
  - [10] C. Ishizuka, T. Suda, H. Suzuki, A. Ohnishi, K. Sumiyoshi and H. Toki, Publ. Astron. Soc. Jap. **67**, 13 (2015), [arXiv:1408.6230 [nucl-th]].
  - [11] C. Gonzalez-Boquera, M. Centelles, X. Viñas and L. M. Robledo, Phys. Lett. B **779**, 195 (2018), [arXiv:1712.06735 [nucl-th]].
  - [12] M. Farine, D. Von-Eiff, P. Schuck, J. F. Berger, J. Decharge, and M. Girod, J. Phys. G **25**, 863 (1999).
  - [13] C. Gonzalez-Boquera, M. Centelles, X. Viñas and A. Rios, Phys. Rev. C **96**, no. 6, 065806 (2017), [arXiv:1706.02736 [nucl-th]].
  - [14] M. Oertel, M. Hempel, T. Klähn and S. Typel, Rev. Mod. Phys. **89**, no. 1, 015007 (2017), [arXiv:1610.03361 [astro-ph.HE]].
  - [15] J. Piekarewicz, Phys. Rev. C **76**, 064310 (2007), [arXiv:0709.2699 [nucl-th]].
  - [16] Y. Lim, K. Kwak, C. H. Hyun and C. H. Lee, Phys. Rev. C **89**, no. 5, 055804 (2014), [arXiv:1312.2640 [nucl-th]].
  - [17] R. Sellahewa and A. Rios, Phys. Rev. C **90**, no. 5, 054327 (2014), [arXiv:1407.8138 [nucl-th]].
  - [18] F. J. Fattoyev and J. Piekarewicz, Phys. Rev. Lett. **111**, 162501 (2013), [arXiv:1306.6034 [nucl-th]].
  - [19] A. W. Steiner, M. Prakash, J. M. Lattimer and P. J. Ellis, Phys. Rept. **411**, 325 (2005), [nucl-th/0410066].
  - [20] M. Centelles, X. Roca-Maza, X. Vinas and M. Warda, Phys. Rev. C **82**, 054314 (2010), [arXiv:1010.5396 [nucl-th]].
  - [21] C. Ducoin, J. Margueron and C. Providencia, EPL **91**, no. 3, 32001 (2010), [arXiv:1004.5197 [nucl-th]].
  - [22] M. Fortin, C. Providencia, A. R. Raduta, F. Gulminelli, J. L. Zdunik, P. Haensel and M. Bejger, Phys. Rev. C **94**, no. 3, 035804 (2016), [arXiv:1604.01944 [astro-ph.SR]].
  - [23] M. Dutra, O. Loureco, J. S. Sa Martins, A. Delfino, J. R. Stone and P. D. Stevenson, Phys. Rev. C **85**, 035201 (2012), [arXiv:1202.3902 [nucl-th]].
  - [24] B. A. Brown and A. Schwenk, Phys. Rev. C **89**, no. 1, 011307 (2014), Erratum: [Phys. Rev. C **91**, no. 4, 049902 (2015)]. [arXiv:1311.3957 [nucl-th]].
  - [25] B. A. Brown, Phys. Rev. Lett. **85**, 5296 (2000).
  - [26] P.-G. Reinhard, A. S. Umar, P. D. Stevenson, J. Piekarewicz, V. E. Oberacker and J. A. Maruhn, Phys. Rev. C **93**, no. 4, 044618 (2016), [arXiv:1603.01319 [nucl-th]].

- [27] Z. Zhang, Y. Lim, J. W. Holt and C. M. Ko, Phys. Lett. B **777**, 73 (2018) doi:10.1016/j.physletb.2017.12.012 [arXiv:1703.00866 [nucl-th]].
- [28] P. W. Zhao and S. Gandolfi, Phys. Rev. C **94**, no. 4, 041302 (2016), [arXiv:1604.01490 [nucl-th]].
- [29] Y. Wang, C. Guo, Q. Li, H. Zhang, Y. Leifels and W. Trautmann, Phys. Rev. C **89**, no. 4, 044603 (2014) doi:10.1103/PhysRevC.89.044603 [arXiv:1403.7041 [nucl-th]].
- [30] L. W. Chen, C. M. Ko, B. A. Li and J. Xu, Phys. Rev. C **82**, 024321 (2010), [arXiv:1004.4672 [nucl-th]].
- [31] O. Lourenco, M. Bhuyan, C. H. Lenzi, M. Dutra, C. Gonzalez-Boquera, M. Centelles and X. Viñas, arXiv:2002.06242 [nucl-th].
- [32] J. Birkhan *et al.*, Phys. Rev. Lett. **118**, no. 25, 252501 (2017), [arXiv:1611.07072 [nucl-ex]].
- [33] M. Tanaka *et al.*, to be published in Phys. Rev. Lett. arXiv:1911.05262 [nucl-ex].
- [34] C. J. Horowitz, Annals Phys. **411**, 167992 (2019), [arXiv:1911.00411 [astro-ph.HE]].
- [35] A. Bauswein, O. Just, H-T. Janka, N. Stergioulas, Astro. Phys. Jour. Let. **850**, 2 (2017), [arXiv:1604.01944[astro-ph.HE]].
- [36] B. D. Metzger, Living Rev. Relativ. **20**, 3 (2017), [arXiv:1610.09381[astro-ph.HE]].
- [37] B. P. Abbott et al. (Virgo, LIGO Scientific), Phys. Rev. Lett. **119**, 161101 (2017).
- [38] F. J. Fattoyev, J. Piekarewicz, and C. J. Horowitz, Phys. Rev. Lett. **120**, 172702 (2018).
- [39] G. Baym, C. Pethick and P. Sutherland, Astrophys. J. **170**, 299 (1971).
- [40] S. Tagami, M. Tanaka, M. Takechi, M. Fukuda and M. Yahiro, Phys. Rev. C **101**, no. 1, 014620 (2020), [arXiv:1911.05417 [nucl-th]].
- [41] A. Tamii *et al.*, Phys. Rev. Lett. **107**, 062502 (2011).
- [42] A. Klimkiewicz *et al.*, Phys. Rev. C **76**, 051603 (2007).
- [43] A. Ong, J. C. Berengut and V. V. Flambaum, Phys. Rev. C **82**, 014320 (2010), [arXiv:1006.5508 [nucl-th]].

TABLE I. Properties of 206 EoSs (1). The symbol  $\ddagger$  is our results, while  $\dagger$  denotes the results of self-consistent calculations.

	m*/m	K	J	L	Ksym	Rskin-208	Rskin-48	Refs.
APR, E0019		266.000	32.600	57.600		0.160	0.160 $\dagger$	[7, 10, 25]
BHF-1		195.500	34.300	66.550	-31.300	0.200 $\ddagger$	0.183 $\dagger$	[21]
BSk14	0.800	239.380	30.000	43.910	-152.030	0.164 $\ddagger$	0.162 $\dagger$	[21, 23]
BSk16	0.800	241.730	30.000	34.870	-187.390	0.149 $\ddagger$	0.154 $\dagger$	[21, 23]
BSk17	0.800	241.740	30.000	36.280	-181.860	0.151 $\dagger$	0.156 $\dagger$	[21, 23]
BSk20	0.800	241.400	30.000	37.400	-136.500	0.153 $\ddagger$	0.157 $\dagger$	[22, 23]
BSk21	0.800	245.800	30.000	46.600	-37.200	0.168 $\dagger$	0.165 $\dagger$	[22, 23]
BSk22		245.900	32.000	68.500	13.000	0.204 $\ddagger$	0.185 $\dagger$	[22]
BSk23		245.700	31.000	57.800	-11.300	0.186 $\dagger$	0.175 $\dagger$	[10, 22]
BSk24		245.500	30.000	46.400	-37.600	0.168 $\dagger$	0.165 $\dagger$	[22]
BSk25		236.000	29.000	36.900	-28.500	0.152 $\ddagger$	0.156 $\dagger$	[22]
BSk26		240.800	30.000	37.500	-135.600	0.153 $\ddagger$	0.157 $\dagger$	[22]
BSR2		239.900	31.500	62.000	-3.100	0.193 $\dagger$	0.179 $\dagger$	[22]
BSR6		235.800	35.600	85.700	-49.600	0.231 $\dagger$	0.200 $\dagger$	[22]
D1		229.400	30.700	18.360	-274.600	0.122 $\dagger$	0.139 $\dagger$	[13]
D1AS		229.400	31.300	66.550	-89.100	0.200 $\dagger$	0.183 $\dagger$	[13]
D1M	0.746 $\ddagger$	224.958 $\ddagger$	28.552 $\ddagger$	24.966 $\ddagger$	-133.692 $\ddagger$	0.113 $\ddagger$	0.147 $\ddagger$	[11]
D1M*	0.746 $\ddagger$	225.365 $\ddagger$	30.249 $\ddagger$	43.311 $\ddagger$	-47.793 $\ddagger$	0.134 $\ddagger$	0.158 $\ddagger$	[11]
D1MK	0.746 $\ddagger$	225.400 $\ddagger$	33.000 $\ddagger$	55.000 $\ddagger$	-37.275 $\ddagger$	0.158 $\ddagger$	0.171 $\ddagger$	TW
D1N	0.748 $\ddagger$	225.525 $\ddagger$	29.594 $\ddagger$	33.665 $\ddagger$	-168.750 $\ddagger$	0.144 $\ddagger$	0.171 $\ddagger$	[11]
D1P	0.672 $\ddagger$	250.860 $\ddagger$	32.418 $\ddagger$	49.827 $\ddagger$	-157.419 $\ddagger$	0.179 $\ddagger$	0.157 $\ddagger$	[12, 13]
D1PK	0.700 $\ddagger$	260.000 $\ddagger$	33.000 $\ddagger$	55.000 $\ddagger$	-150.000 $\ddagger$	0.182 $\ddagger$	0.181 $\ddagger$	TW
D1S	0.697 $\ddagger$	202.856 $\ddagger$	31.125 $\ddagger$	22.558 $\ddagger$	-241.797 $\ddagger$	0.137 $\ddagger$	0.159 $\ddagger$	[9, 11]
D2	0.738	209.300	31.130	44.850		0.165 $\dagger$	0.163 $\dagger$	[11]
D250		249.900	31.570	24.820	-289.400	0.133 $\dagger$	0.145 $\dagger$	[13]
D260		259.500	30.110	17.570	-298.700	0.121 $\dagger$	0.139 $\dagger$	[13]
D280		285.200	33.140	46.530	-211.900	0.168 $\dagger$	0.165 $\dagger$	[13]
D300		299.100	31.220	25.840	-315.100	0.135 $\dagger$	0.146 $\dagger$	[13]
DD		241.000	31.700	56.000	-95.000	0.183 $\dagger$	0.173 $\dagger$	[30]
DD-F		223.000	31.600	56.000	-140.000	0.183 $\dagger$	0.173 $\dagger$	[30]
DD-ME1		245.000	33.100	55.000	-101.000	0.203 $\dagger$	0.193 $\dagger$	[10, 21, 28, 30]
DD-ME2		251.000	32.300	51.240	-87.000	0.203 $\dagger$	0.187 $\dagger$	[21, 22, 28, 30]
DD-PC1				67.799		0.203 $\dagger$	0.195 $\dagger$	[21, 28]
Ducoin		240.200	32.760	55.300	-124.700	0.182 $\dagger$	0.173 $\dagger$	[21]
E0008(TMA)		318.000	30.660	90.140		0.239 $\dagger$	0.204 $\dagger$	[10]
E0009		280.000	32.500	88.700		0.236 $\dagger$	0.203 $\dagger$	[10, 14]
E0015		216.700	30.030	45.780		0.167	0.164	[10]
E0024		244.500	33.100	55.000		0.182 $\dagger$	0.172	[10]
E0025		211.000	31.600	107.400		0.267 $\dagger$	0.220 $\dagger$	[10]
E0036		281.000	36.900	110.800		0.272 $\dagger$	0.223 $\dagger$	[10]
es25		211.730	25.000	27.749 $\dagger$		0.138	0.148 $\dagger$	[19]
es275		205.330	27.500	48.549 $\dagger$		0.171	0.167 $\dagger$	[19, 22]
es30		215.360	30.000	69.603 $\dagger$		0.205	0.186 $\dagger$	[19]
es325		212.450	32.500	81.925 $\dagger$		0.225	0.197 $\dagger$	[19]
es35		209.970	34.937	96.182 $\dagger$		0.248	0.210 $\dagger$	[19]
FKVW		379.000	33.100	80.000	11.000	0.222 $\dagger$	0.195 $\dagger$	[30]
FSU		230.000	32.590	60.500	-51.300	0.210	0.188 $\dagger$	[18, 21]
FSUgold		229.000	32.500	60.000	-52.000	0.210	0.200	[14, 15, 30]
FSUgold2.1		230.000	32.590	60.500		0.191 $\dagger$	0.177 $\dagger$	[10, 14]
GM1		299.700	32.480	93.870	17.890	0.245 $\dagger$	0.207 $\dagger$	[21, 22]
GM3		239.900	32.480	89.660	-6.470	0.238 $\dagger$	0.204 $\dagger$	[21]
Gs		237.570	31.384	89.304 $\dagger$		0.237	0.203 $\dagger$	[19]
GSKI		230.210	32.030	63.450	-95.290	0.195 $\dagger$	0.180 $\dagger$	[23]
GSKII	0.790	233.400	30.490	48.630	-157.830	0.171 $\dagger$	0.167 $\dagger$	[23]
GT2		228.100	33.940	5.020	-445.900	0.101 $\dagger$	0.127 $\dagger$	[13]
G $\sigma$		237.290	31.370	94.020	13.990	0.245 $\dagger$	0.208 $\dagger$	[21]
HA		233.000	30.700	55.000	-135.000	0.182 $\dagger$	0.172 $\dagger$	[30]
HFB-17				36.300		0.151	0.155 $\dagger$	[2]
HFB-8				14.800		0.115	0.135 $\dagger$	[2]
HS(DD2)		243.000	31.700	55.000	-93.200	0.182 $\dagger$	0.172 $\dagger$	[14, 22]
IU-FSU		231.200	31.300	47.200	28.700	0.160	0.160 $\dagger$	[14, 18]
KDE0v1	0.740	227.540	34.580	54.690	-127.120	0.181 $\dagger$	0.172 $\dagger$	[23]
KDE0v1-B	0.790	216.000	34.900	61.000		0.192	0.172	[24]
KDE0v1-T	0.810	217.000	34.600	72.000	-40.000	0.200	0.178	[8]

TABLE I. Properties of 206 EoSs (2).

	m*/m	K	J	L	Ksym	Rskin-208	Rskin-48	Refs.
LNS	0.830	210.780	33.430	61.450	-127.360	0.192 <sup>†</sup>	0.178 <sup>†</sup>	[21, 23]
LS180		180.000	28.600	73.800		0.212 <sup>†</sup>	0.189 <sup>†</sup>	[10, 14, 23]
LS220		220.000	28.600	73.800		0.212 <sup>†</sup>	0.189 <sup>†</sup>	[10, 14, 23]
LS375		375.000	28.600	73.800		0.212 <sup>†</sup>	0.189 <sup>†</sup>	[10, 14, 23]
Ly5		229.940	32.010	45.243 <sup>†</sup>		0.166	0.164 <sup>†</sup>	[19]
M3Y-P6		239.700	32.100	44.600	-165.300	0.165 <sup>†</sup>	0.163 <sup>†</sup>	[9, 16]
M3Y-P7		254.700	31.700	51.500	-127.800	0.176 <sup>†</sup>	0.169 <sup>†</sup>	[9, 22]
MSk3	1.000	233.250	28.000	7.040	-283.520	0.111	0.128	[23, 28]
MSk6	1.050	231.170	28.000	9.630	-274.330	0.118	0.130	[23, 28]
MSk7	1.050	385.360	27.950	9.400	-274.630	0.116	0.136 <sup>†</sup>	[2, 23]
MSL0	0.800	230.000	30.000	60.000	-99.330	0.180	0.171 <sup>†</sup>	[23, 29, 30]
NL1		212.000	43.500	140.000	143.000	0.319	0.247	[28, 30]
NL2		401.000	44.000	130.000	20.000	0.304	0.243	[28, 30]
NL3		271.000	37.300	118.000	100.000	0.280	0.230	[15, 18, 20–22, 30]
NL3*				119.769 <sup>†</sup>		0.287	0.230	[28]
NL3 $\omega\rho$		271.600	31.700	55.500	-7.600	0.183 <sup>†</sup>	0.173 <sup>†</sup>	[22]
NL4		270.350	36.239	111.649 <sup>†</sup>		0.273	0.223 <sup>†</sup>	[19]
NL-SH		356.000	36.100	114.000	80.000	0.263	0.214	[28, 30]
NL $\rho$		240.000	30.300	85.000	3.000	0.230 <sup>†</sup>	0.199 <sup>†</sup>	[30]
NL $\omega\rho(025)$		270.700	32.350	61.050	-34.360	0.192 <sup>†</sup>	0.178 <sup>†</sup>	[21]
NRAPR	0.690	225.700	32.787	59.630	-123.320	0.190	0.177 <sup>†</sup>	[19, 23]
NRAPR-B	0.850	225.000	35.100	61.000		0.193	0.178	[24]
NRAPR-T	0.730	221.000	34.100	70.000	-46.000	0.195	0.181	[8]
PC-F1		255.000	37.800	117.000	75.000	0.269	0.225	[28, 30]
PC-F2		256.000	37.600	116.000	65.000	0.281 <sup>†</sup>	0.227 <sup>†</sup>	[28–30]
PC-F3		256.000	38.300	119.000	74.000	0.285 <sup>†</sup>	0.230 <sup>†</sup>	[28, 30]
PC-F4		255.000	37.700	119.000	98.000	0.285 <sup>†</sup>	0.230 <sup>†</sup>	[30]
PC-LA		263.000	37.200	108.000	-61.000	0.268 <sup>†</sup>	0.220 <sup>†</sup>	[30]
PC-PK1				101.478		0.257	0.220	[28]
PK1		282.000	37.600	116.000	55.000	0.277	0.223	[28, 30]
PKDD		263.000	36.900	90.000	-80.000	0.253	0.214	[28, 30]
RAPR		276.700	33.987	66.958 <sup>†</sup>		0.201	0.183 <sup>†</sup>	[19]
RATP		239.580	29.260	32.390	-191.250	0.145 <sup>†</sup>	0.152 <sup>†</sup>	[21]
rDD-ME2				51.300		0.193	0.179 <sup>†</sup>	[2]
rFSUGold				60.500		0.207	0.186 <sup>†</sup>	[2, 22]
rG2				100.700		0.257	0.214 <sup>†</sup>	[2]
rNL1				140.100		0.321	0.250 <sup>†</sup>	[2]
rNL3				118.500		0.280	0.227 <sup>†</sup>	[2]
rNL3*				122.600		0.288	0.232 <sup>†</sup>	[2]
rNLC				108.000		0.263	0.218 <sup>†</sup>	[2]
rNL-RA1				115.400		0.274	0.224 <sup>†</sup>	[2]
rNL-SH				113.600		0.266	0.219 <sup>†</sup>	[2]
rNL-Z				133.300		0.307	0.242 <sup>†</sup>	[2]
Rs		237.660	30.593	80.096 <sup>†</sup>	-9.100	0.222	0.195 <sup>†</sup>	[19, 22]
rTM1				110.800		0.271	0.222 <sup>†</sup>	[2]
R $\sigma$		237.410	30.580	85.700	-9.130	0.231 <sup>†</sup>	0.200 <sup>†</sup>	[21]
S271		271.000	35.927	97.541 <sup>†</sup>		0.251	0.211 <sup>†</sup>	[19]
SFH <sub>o</sub>		245.000	31.600	47.100		0.169 <sup>†</sup>	0.165 <sup>†</sup>	[14]
SFH <sub>x</sub>		239.000	28.700	23.200		0.130 <sup>†</sup>	0.144 <sup>†</sup>	[14]
SGI	0.610	262.000	28.300	63.900	-51.990	0.196 <sup>†</sup>	0.180 <sup>†</sup>	[16, 19, 23]
SGII	0.790	214.700	26.830	37.620	-145.920	0.136	0.147 <sup>†</sup>	[2, 9, 21, 23]
SII	0.580	341.400	34.160	50.020	-265.720	0.196	0.177	[28]
SIII	0.760	355.37	28.160	9.910	-393.730	0.137	0.125	[23, 28]
Sk $\chi$ m		230.400	30.940	45.600		0.167	0.164 <sup>†</sup>	[23, 27]
SK255		254.960	37.400	95.000	-58.300	0.247 <sup>†</sup>	0.208 <sup>†</sup>	[22]
SK272		271.550	37.400	91.700	-67.800	0.241 <sup>†</sup>	0.205 <sup>†</sup>	[22]
Ska	0.610	263.160	32.910	74.620	-78.460	0.214 <sup>†</sup>	0.190 <sup>†</sup>	[2, 9, 14, 22, 23, 29]
Ska25-B	0.990	219.000	32.500	51.000		0.176	0.170	[24]
Ska25s20	0.980	220.750	33.780	63.810	-118.220	0.196 <sup>†</sup>	0.180 <sup>†</sup>	[23]
Ska25-T	0.980	220.000	31.900	59.000	-59.000	0.183	0.176	[8]
Ska35-B	1.000	244.000	32.800	54.000		0.180	0.172	[24]
Ska35s20	1.000	240.270	33.570	64.830	-120.320	0.198 <sup>†</sup>	0.181 <sup>†</sup>	[23, 29]
Ska35-T	0.990	238.000	32.000	58.000	-84.000	0.184	0.177	[8, 21, 23]

TABLE I. Properties of 206 EoSs (3).

	m*/m	K	J	L	Ksym	Rskin-208	Rskin-48	Refs.
SKb	0.610	263.000	33.880	47.600	-78.500	0.170 <sup>†</sup>	0.166 <sup>†</sup>	[22, 23]
SkI1	0.690	242.750	37.530	161.050	234.670	0.353 <sup>†</sup>	0.268 <sup>†</sup>	[23, 29]
SkI2	0.680	240.700	33.400	104.300	70.600	0.262 <sup>†</sup>	0.217 <sup>†</sup>	[9, 21–23]
SkI3	0.580	258.000	34.800	100.500	72.900	0.255 <sup>†</sup>	0.213 <sup>†</sup>	[9, 21–23]
SkI4	0.650	247.700	29.500	60.400	-40.600	0.191 <sup>†</sup>	0.177 <sup>†</sup>	[9, 16, 21–23]
SkI5	0.580	255.800	36.697	129.300	159.500	0.272	0.214	[9, 19, 21–23]
SkI6	0.640	248.650	30.090	59.700	-47.270	0.189 <sup>†</sup>	0.177 <sup>†</sup>	[21–23]
SkM*	0.790	216.610	30.030	45.780	-155.940	0.170	0.155	[2, 9, 23, 28]
SkM*-B	0.780	218.000	34.200	58.000		0.187	0.175	[24]
SkM*-T	0.790	219.000	33.700	65.000	-65.000	0.187	0.179	[8]
SkMP	0.650	230.930	29.890	70.310	-49.820	0.197	0.167	[2, 19, 21, 22]
SkO	0.900	223.390	31.970	79.140	-43.170	0.221 <sup>†</sup>	0.194 <sup>†</sup>	[21, 23]
SKOp	0.900	222.360	31.950	68.940	-78.820	0.204 <sup>†</sup>	0.185 <sup>†</sup>	[22, 23]
SKP	1.000	200.970	30.000	19.680	-266.600	0.144	0.144	[23, 28]
SKRA	0.750	216.980	31.320	53.040	-139.280	0.179 <sup>†</sup>	0.171 <sup>†</sup>	[23]
SKRA-B	0.790	212.000	33.700	55.000		0.181	0.172	[23, 24]
SKRA-T	0.800	213.000	33.400	65.000	-55.000	0.190	0.179	[8, 23]
Sk-Rs			85.700			0.215	0.191 <sup>†</sup>	[2]
SkSM*			65.500			0.197	0.181 <sup>†</sup>	[2]
SkT1	1.000	236.160	32.020	56.180	-134.830	0.184 <sup>†</sup>	0.173 <sup>†</sup>	[23]
SkT1-B	0.970	242.000	33.300	56.000		0.183	0.172	[24]
SkT1-T	0.970	238.000	32.600	63.000	-70.000	0.190	0.179	[8, 23]
SkT2	1.000	235.730	32.000	56.160	-134.670	0.184 <sup>†</sup>	0.173 <sup>†</sup>	[23]
SkT2-B	0.970	242.000	33.500	58.000		0.186	0.174	[24]
SkT2-T	0.960	238.000	32.600	62.000	-75.000	0.188	0.178	[8, 23]
SkT3	1.000	235.740	31.500	55.310	-132.050	0.182 <sup>†</sup>	0.173 <sup>†</sup>	[23]
SkT3-B	0.980	241.000	32.700	53.000		0.179	0.172	[24]
SkT3-T	0.970	236.000	31.900	58.000	-80.000	0.183	0.178	[8]
Sk-T4	1.000	235.560	35.457	94.100	-24.500	0.253	0.212 <sup>†</sup>	[2, 9, 19]
Sk-T6	1.000	235.950	29.970	30.900	-211.530	0.151	0.155 <sup>†</sup>	[2, 23]
Skxs20	0.960	201.950	35.500	67.060	-122.310	0.201 <sup>†</sup>	0.183 <sup>†</sup>	[23]
Skz2	0.700	230.070	32.010	16.810	-259.660	0.120 <sup>†</sup>	0.138 <sup>†</sup>	[23, 29]
Skz4	0.700	230.080	32.010	5.750	-240.860	0.102 <sup>†</sup>	0.128 <sup>†</sup>	[23, 29]
SLy0	0.700	229.670	31.982	44.873 <sup>†</sup>	-116.230	0.165	0.163 <sup>†</sup>	[19, 23]
SLy10	0.680	229.740	31.980	38.740	-142.190	0.155 <sup>†</sup>	0.158 <sup>†</sup>	[21, 23]
Sly2	0.700	229.920	32.000	47.460	-115.130	0.170 <sup>†</sup>	0.166 <sup>†</sup>	[22, 23]
SLy230a	0.700	229.890	31.980	44.310	-98.210	0.155	0.158 <sup>†</sup>	[19, 21–23]
SLy230b	0.690	229.960	32.010	45.960	-119.720	0.167 <sup>†</sup>	0.164 <sup>†</sup>	[21, 23]
SLy4	0.690	229.900	32.000	45.900	-119.700	0.162	0.152	[2, 9, 11, 16, 22, 28]
SLy4-B	0.700	224.000	34.100	56.000		0.184	0.174	[24]
SLy4-T	0.760	222.000	33.600	66.000	-55.000	0.191	0.179	[8, 23]
SLy5	0.700	229.920	32.010	48.150	-112.760	0.162	0.160	[23, 28]
SLy6	0.690	229.860	31.960	47.450	-112.710	0.161	0.152	[23, 28]
Sly9	0.670	229.840	31.980	54.860	-81.420	0.182 <sup>†</sup>	0.172 <sup>†</sup>	[22, 23]
SQMC650	0.780	218.110	33.650	52.920	-173.150	0.178 <sup>†</sup>	0.171 <sup>†</sup>	[23]
SQMC700	0.760	222.200	33.470	59.060	-140.840	0.188 <sup>†</sup>	0.176 <sup>†</sup>	[23]
SQMC750-B	0.710	228.000	34.800	59.000		0.190	0.176	[24]
SQMC750-T	0.750	223.000	33.900	68.000	-50.000	0.194	0.180	[8, 23]
SR1	0.900	202.150	29.000	41.245 <sup>†</sup>		0.160	0.160 <sup>†</sup>	[19]
SR2		224.640	30.071	49.130 <sup>†</sup>		0.172	0.167 <sup>†</sup>	[19]
SR3		222.550	29.001	48.308 <sup>†</sup>		0.171	0.166 <sup>†</sup>	[19]
SV	0.380	306.000	32.800	96.100	24.190	0.230	0.196	[16, 21, 23, 28]
SV-bas	0.900	221.760	30.000	32.000	-156.570	0.155	0.158 <sup>†</sup>	[23, 26]
SV-K218	0.900	218.230	30.000	35.000	-206.870	0.161	0.161 <sup>†</sup>	[23, 26]
SV-K226	0.900	225.820	30.000	34.000	-211.920	0.159	0.160 <sup>†</sup>	[23, 26]
SV-K241	0.900	241.070	30.000	31.000	-230.770	0.151	0.155 <sup>†</sup>	[23, 26]
SV-kap00	0.900	233.440	30.000	40.000	-161.780	0.158	0.159 <sup>†</sup>	[23, 26]
SV-kap20	0.900	233.440	30.000	36.000	-193.190	0.155	0.158 <sup>†</sup>	[23, 26]
SV-kap60	0.900	233.450	30.000	29.000	-249.750	0.154	0.157 <sup>†</sup>	[23, 26]
SV-L25	0.900		30.000	25.000		0.143	0.151 <sup>†</sup>	[26]
SV-L32	0.900		30.000	32.000		0.154	0.157 <sup>†</sup>	[26]
SV-L40	0.900	233.3	30.000	40.000		0.166	0.164 <sup>†</sup>	[26]
SV-L47	0.900	233.4	30.000	47.000		0.177	0.170 <sup>†</sup>	[26]

TABLE I. Properties of 206 EoSs (4).

	m*/m	K	J	L	Ksym	Rskin-208	Rskin-48	Refs.
SV-mas07	0.700	233.540	30.000	52.000	-98.770	0.152	0.156 <sup>†</sup>	[23, 26]
SV-mas08	0.800	233.130	30.000	40.000	-172.380	0.160	0.160 <sup>†</sup>	[23, 26, 29]
SV-mas10	1.000	234.330	30.000	28.000	-252.500	0.152	0.156 <sup>†</sup>	[23, 26]
SV-sym28	0.900	240.860	28.000	7.000	-305.940	0.117	0.136 <sup>†</sup>	[23, 26]
SV-sym32	0.900	233.810	32.000	57.000	-148.790	0.192	0.178 <sup>†</sup>	[23, 26]
SV-sym32-B	0.910	237.000	32.300	51.000		0.176	0.174	[24]
SV-sym32-T	0.910	232.000	31.500	58.000	-77.000	0.181	0.179	[8]
SV-sym34	0.900	234.070	34.000	81.000	-79.080	0.227	0.198 <sup>†</sup>	[23, 26, 29]
TFa		245.100	35.050	82.500	-68.400	0.250	0.210 <sup>†</sup>	[18]
TFb		250.100	40.070	122.500	45.800	0.300	0.238 <sup>†</sup>	[18]
TFc		260.500	43.670	135.200	51.600	0.330	0.255 <sup>†</sup>	[18]
TM1		281.000	36.900	110.800	33.550	0.272 <sup>†</sup>	0.223 <sup>†</sup>	[10, 21, 22, 30]
TW99		241.000	32.800	55.000	-124.000	0.196	0.186	[28, 30]
UNEDF0		229.800	30.500	45.100	-189.600	0.166 <sup>†</sup>	0.164 <sup>†</sup>	[9, 23]
UNEDF1		219.800	29.000	40.000	-179.400	0.158 <sup>†</sup>	0.159 <sup>†</sup>	[9]
Z271		271.000	35.369	89.520 <sup>†</sup>		0.238	0.204 <sup>†</sup>	[19]

TABLE II. Parameter sets of D1MK and D1PK.

D1MK	$\mu_i$	$W_i$	$B_i$	$H_i$	$M_i$	$t_0^i$	$x_0^i$	$\alpha_i$	$W_0$
$i = 1$	0.5	-17242.0144	19604.4056	-20699.9856	16408.6002	1561.7167	1	1/3	115.36
$i = 2$	1.0	642.607965	-941.150253	865.572486	-845.300794	0	-1	1	
D1PK	$\mu_i$	$W_i$	$B_i$	$H_i$	$M_i$	$t_0^i$	$x_0^i$	$\alpha_i$	$W_0$
$i = 1$	0.90	-465.027582	155.134492	-506.775323	117.749903	981.065351	1	1/3	130
$i = 2$	1.44	34.6200000	-14.0800000	70.9500000	-41.3518104	534.155654	-1	1	

TABLE III. Properties of 47 EoSs satisfying the observational constraint.

	J	L	Ksym	R-max	M-max	Refs.
APR, E0019	32.60	57.60		10.0	2.20	[7, 10, 25]
BSk20	30.00	37.40	-136.50	10.2	2.17	[22, 23]
BSk21	30.00	46.60	-37.20	11.0	2.29	[22, 23]
BSk22	32.00	68.50	13.00	11.2	2.27	[22]
BSk23	31.00	57.80	-11.30	11.2	2.28	[10, 22]
BSk24	30.00	46.40	-37.60	11.2	2.29	[22]
BSk25	29.00	36.90	-28.50	11.2	2.23	[22]
BSk26	30.00	37.50	-135.60	10.2	2.18	[22]
BSR2	31.50	62.00	-3.10	11.9	2.38	[22]
BSR6	35.60	85.70	-49.60	12.1	2.44	[22]
D1AS	31.30	66.55	-89.10	10.0	2.00	[13]
D1M*	30.25	43.15	-47.79	9.6	2.00	[11, 31]
D1PK	33.00	55.00	-150.00	10.0	2.1	TW
D2	31.13	44.85		10.2	2.1	[11, 31]
DD-ME1	33.10	55.00		11.9	2.47	[10, 21, 28, 30]
DD-ME2	32.30	51.20	-87.00	12.2	2.48	[21, 22, 28, 30]
E0008(TMA)	30.66	90.14		12.4	2.04	[10]
FSUgold2.1	32.60	60.50		12.1	2.13	[10, 14]
GM1	32.50	94.40	17.89	12.0	2.36	[21, 22]
HS(DD2)	31.70	55.00	-93.20	11.8	2.42	[14, 22]
LS220	28.60	73.80		10.6	2.05	[10, 14, 23]
LS375	28.60	73.80		12.6	2.72	[10, 14, 23]
NL3	37.30	118.00	100.00	13.3	2.77	[15, 18, 20–22, 30]
NL3 $\omega\rho$	31.70	55.50	-7.60	13.0	2.75	[22]
Rs	30.59	80.06	-9.10	10.8	2.12	[19, 22]
SFH <sub>0</sub>	31.60	47.10		10.5	2.05	[14]
SFH <sub>x</sub>	28.70	23.20		10.9	2.14	[14]
SGI	28.30	63.90	-51.99	12.0	2.25	[16, 19, 22, 23]
SK255	37.40	95.00	-58.30	11.0	2.15	[22]
SK272	37.40	91.70	-67.80	11.2	2.24	[22]
SKa	32.91	74.62	-78.46	11.0	2.21	[2, 9, 14, 22, 23, 29]
SKb	33.88	47.60	-78.50	10.6	2.2	[22, 23]
SkI2	33.40	104.30	70.60	11.3	2.17	[9, 21–23]
SkI3	34.80	100.50	72.90	11.4	2.25	[9, 21–23]
SkI4	29.50	60.40	-40.60	10.6	2.18	[9, 16, 21–23]
SKi5	36.70	129.30	159.50	11.3	2.25	[9, 19, 21–23]
SkI6	30.09	59.70	-47.27	11.2	2.2	[9, 19, 21–23]
SkMP	29.89	70.31	-49.82	10.8	2.11	[2, 21? , 22]
Sly2	32.00	47.46	-115.13	10.0	2.06	[22, 23]
Sly230a	31.98	44.31	-98.21	10.3	2.11	[19, 21–23]
SLy4	32.00	45.90	-119.70	10.0	2.06	[2, 9, 11, 16, 22, 28]
Sly9	31.98	54.86	-81.42	10.6	2.16	[22, 23]
SV	32.80	96.10		11.7	2.44	[16, 21, 23, 28]
TFa	35.05	82.50		12.2	2.10	[18]
TFb	40.07	122.50		12.6	2.15	[18]
TFc	43.67	135.20		12.9	2.21	[18]
TM1	36.90	110.80		12.5	2.18	[10, 21, 22, 30]